

# Clinical heterogeneity in retinitis pigmentosa caused by variants in *RPI* and *RLBPI* in five extended consanguineous pedigrees

Muawyah Al-Bdour,<sup>1</sup> Svenja Pauleck,<sup>2</sup> Zain Dardas,<sup>3</sup> Raghda Barham,<sup>4</sup> Dema Ali,<sup>4</sup> Sami Amr,<sup>5</sup> Lina Mustafa,<sup>3</sup> Mohammed Abu-Ameerh,<sup>1</sup> Ranad Maswadi,<sup>6</sup> Belal Azab,<sup>3,7,8</sup> Abdalla Awidi<sup>4,9</sup>

<sup>1</sup>Ophthalmology Department, Jordan University Hospital, The University of Jordan, Amman, Jordan; <sup>2</sup>Medical Department, The University of Leipzig, Germany; <sup>3</sup>Department of Pathology, Microbiology and Forensic Medicine, School of Medicine, The University of Jordan, Amman, Jordan; <sup>4</sup>Cell Therapy Center, The University of Jordan, Amman, Jordan; <sup>5</sup>Department of Pathology, Brigham and Women's Hospital, Harvard Medical School, Boston, MA; <sup>6</sup>Department of Ophthalmology St Thomas' Hospital, London, UK; <sup>7</sup>Department of Human and Molecular Genetics, Medical College of Virginia, Virginia Commonwealth University, Richmond, VA; <sup>8</sup>Prevention Genetics, Marshfield, WI; <sup>9</sup>Department of Medicine and Hematology, Jordan University Hospital, The University of Jordan, Amman, Jordan

**Purpose:** The aim of this study is to identify disease-causing variants in five consanguineous Jordanian families with a history of autosomal recessive retinitis pigmentosa (RP), and to investigate the clinical variability across the affected individuals.

**Methods:** Exome sequencing (ES) and ophthalmic examinations were performed to classify the underlying RP-causative variants and their pathogenic consequences. The candidate variants in the affected and unaffected family members underwent segregation analyses with Sanger sequencing.

**Results:** We described four variants in the *RPI* and *RLBPI* genes as disease-causing across the five families, including novel (c.398delC; p.Pro133GlnfsTer126) and recurrent (c.79delA; p.Thr27ProfsTer26) variants in *RLBPI* and two previously reported variants in *RPI* ((c.1126C>T; p.Arg376Ter) and (c.607G>A; p.Gly203Arg)). The consequent clinical manifestations were thoroughly investigated using a battery of ophthalmic tests, including electroretinography (ERG), optical coherence tomography (OCT), visual acuity (VA), and fundus examination. The phenotypes indicated clinical heterogeneity, typical RP for variants in *RPI*, and retinitis punctata albescens (RPA) for variants in *RLBPI*.

**Conclusions:** This study extends the pathogenic variant spectrum for the *RPI* and *RLBPI* genes. The study also revealed the consequent clinical progression, severity, and presentation of RP. Furthermore, we confirm that ES is an efficient molecular diagnostic approach for RP.

Inherited retinal dystrophies (IRDs) include clinically and genetically complex diseases such as retinitis pigmentosa (RP) [1]. RP is the most common degenerative peripheral retinal dystrophy caused by progressive deterioration of photoreceptors [2,3]. The prevalence of RP depends on geographic location and ranges between 1:9,000 [4] and 1:750 [5]. Prevalence increases in ethnic groups that share common ancestors, such as the Jordanian population [6]. During RP preclinical stages, rod degeneration is not often observed through standard clinical examination. Thorough retinal assessment, such as electroretinography (ERG), is required to investigate the disease, especially in its early stages [7]. The first symptoms are night blindness followed by progressive visual field scotomas, decreased visual acuity, and abnormal color vision. RP later advances to cone degeneration, leading to total blindness [8]. The clinical manifestations of deteriorated retinas include attenuated vessels, intraretinal pigment

deposits, and waxy optic disc pallor [9,10]. The clinical presentation varies depending on the penetrance and expressivity of disease-causing genes [11]. RP exhibits phenotypic heterogeneity with a wide range of severity and variable age of onset, ranging from early childhood to late adulthood [12]. It is a complex disease with genetic and allelic heterogeneity [13], and can arise from different modes of inheritance, including autosomal dominant (adRP), autosomal recessive (arRP), X-linked (XLRP), and mitochondrial (mtRP) [14]. Thus far, more than 57 genes with about 3,000 RP-causative variants have been identified [15].

In this study, *RPI* (Gene ID 19888; OMIM 603937) and *RLBPI* (Gene ID 6017; OMIM 180090) were identified through exome sequencing (ES) to cause RP in five consanguineous Jordanian families. ES represents a highly sensitive and efficient strategy for molecular diagnosis in phenotypically and genetically heterogeneous monogenic diseases, such as RP [16], with a detection rate ranging from 36% to 80% [12].

Correspondence to: Belal Azab, Prevention Genetics, 3800 S Business Park Ave, Marshfield, 54449 WI, Phone: (804) 263-2950; email: azabm@mymail.vcu.edu

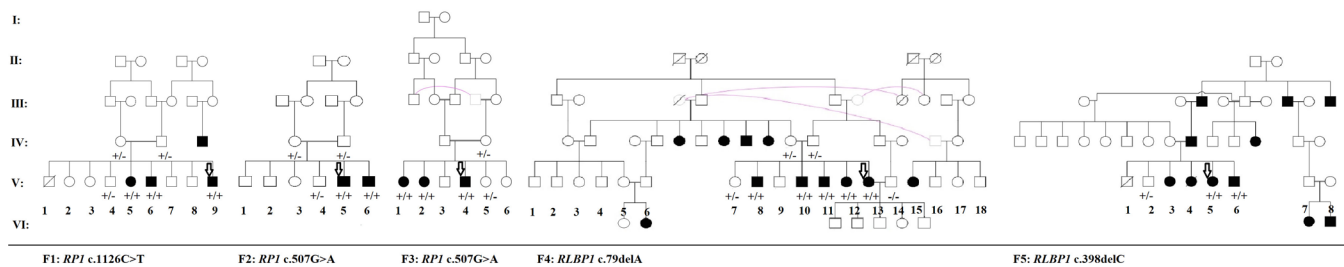


Figure 1. Six-generation pedigrees of the investigated families (F1 to F5). Circles indicate females, and squares indicate males. Filled symbols represent affected members, arrows indicate proband patients in each family, and double lines indicate consanguinity. Pink connected symbols signify the same person. The identified disease-causing variants are noted beneath each pedigree. Families F2 and F3 carry the same identified variants. - indicates the wild-type normal allele, and + indicates the variant allele.

## METHODS

**Patients and clinical examination:** This study was performed according to the principles of the Declaration of Helsinki, following the ARVO statement on human subject studies in Ophthalmic and Vision Research and was approved by the Institutional Review Board of the Cell Therapy Center, The University of Jordan. All participants provided written informed consent. Five extended consanguineous Jordanian families affected by retinal diseases were recruited for the study. Pedigrees F1, F2, and F5 present a first-degree cousin marriage, while pedigrees F3 and F4 have first- and second-degree cousin marriages. Of these families, 12 affected individuals participated as follows: three patients in F1, two patients in F2, one patient in F3, four patients in F4, and two patients in F5. Thirteen unaffected relatives were included as controls: parents and siblings in families F1 to F4 and one sibling in family F5 (Figure 1).

The inclusion criteria for participants were RP-related symptoms, such as night blindness or decreased night vision, low visual acuity, and reduction in ERG amplitudes. Furthermore, the affected individuals underwent ophthalmic examinations, including visual acuity (VA), best-corrected visual acuity (BCVA), slit-lamp biomicroscopy (BM 900; Haag-Streit, Koeniz, Switzerland), dilated fundus examination, fundus photography (200Tx; Optos, Dunfermline, Scotland, UK), optical coherence tomography (OCT) to measure retinal thickness and integrity (Optovue RTVue, Fremont, CA), Pentacam for RP-related keratoconus detection (Pentacam Typ70700; Oculus, Wetzlar, Germany), and full-field flash electroretinograms (ffERGs) to measure photoreceptor electric activity (Color Ganzfeld Q450 C; Roland Consult, Brandenburg an der Havel, Germany). ERGs were recorded following the standards of the International Society for Clinical Electrophysiology of Vision.

**DNA extraction:** Blood samples for molecular genetic testing were collected from affected and unaffected relatives of families F1, F2, F3, F4, and F5. Genomic DNA was extracted from peripheral blood leukocytes using a QIAprep Spin Miniprep Kit (Qiagen GmbH, Duesseldorf, Germany) according to the manufacturer's instructions. The quantity and quality of the extracted DNA were assessed using a NanoDrop 2000 spectrophotometer (Thermo Fisher Scientific, Waltham, MA). The DNA samples were stored at  $-80^{\circ}\text{C}$ .

**Exome sequencing and data analysis**—Exome sequencing was conducted for a single proband from each family. Exome capture was completed using an Agilent Sure Select Human All Exon 65 Mb kit V5 (Agilent, Santa Clara, CA), according to the manufacturer's protocols. The DNA libraries of the probands were sequenced using the HiSeq 2500 platform (Illumina Inc., San Diego, CA) to generate 100-bp paired-end reads at the Partners HealthCare Personalized Medicine (PPM) Translational Genomics Core (Cambridge, MA). Sequence reads were aligned to the human reference genome (GRCh37) using the [Burrows-Wheeler Aligner](#), and variants were called using the Genomic Analysis Tool Kit (GATK). To identify the candidate disease-causing variants, the findings were annotated and filtered against four databases: [NCBI CCDS](#), [RefSeq](#), [Ensembl](#), and [Encode](#). The Variant Call Format (vcf) files were analyzed using the [Illumina](#) basespace variant interpreter tool. The filtered variants were subsequently queried in [ClinVar](#) and the Human Gene Mutation Database ([HGMD](#)). To evaluate the possible deleterious effects of the variants, in silico prediction analyses were performed using Alamut Visual prediction software ([SIFT](#), [MutationTaster](#), and [PolyPhen-2](#)). Alamut annotations were also used to estimate the evolutionary conservation of the respective amino acid positions. The variants were classified according to the interpretation guidelines of the American College of Medical Genetics and Genomics (ACMG).

**Validation and segregation analysis**—Sanger sequencing was used to confirm the pathogenic variants revealed by ES and to perform segregation analysis in affected and unaffected family members. Primers were designed using Primer 3.0 and synthesized by IDT (Appendix 1). Genomic DNA was PCR-amplified using Platinum PCR SuperMix (Invitrogen) with (i) 94 °C for 2 min, (iii) 94 °C for 30 s and 60.0 °C for 15 s and 68 °C for 30 s (35 cycles), (iii) 68 °C for 5 min, and the PCR products were then purified using a GeneJET PCR purification kit (Invitrogen). Sequencing was performed using a BigDye Terminator V3.1 Cycle Sequencing kit (Applied Biosystems, Thermo Fisher Scientific, Waltham, MA) on an ABI 3500 genetic analyzer, and the sequence data were analyzed with SeqA software (Applied Biosystems) and Chromas Pro software (Technelysium LTD, South Brisbane, Australia).

## RESULTS

Five consanguineous Jordanian families were recruited, including 12 individuals between 25 and 60 years affected with RP. Patients underwent thorough ophthalmic examinations; the clinical results are summarized in Table 1, Table 2, and Appendix 2. The five pedigrees were clinically categorized into two phenotypically correlated groups, typical RP and retinitis punctata albescens (RPA), based on the fundus examination, initial symptoms, and disease progression. *RPI* was the candidate underlying disease-causing gene in families F1, F2, and F3 (Figure 1). Disease onset presented as initial symptoms of nyctalopia, between the age of 5 and 10 years. The pathology progressed to peripheral vision loss and central vision loss between 22 and 30 years. However, patient F2-V5, age 27, did not present with central vision loss. Fundus images revealed the typical RP triad of attenuated retinal vessels, intraretinal pigment deposits, and waxy optic disc pallor (Appendix 2). ERG results showed moderate (F1-V6 and F3-V4) and severely reduced electrical responses (F1-V5, F1-V9, F2-V5, and F2-V5; Figure 2). We noticed that the ERG degrees of severity did not correlate with the patients' decreased VAs. The VAs for F1 and F3 members were light perception (LP) or hand motion (HM), with a central vision loss at the ages of 25 and 22, respectively. However, only the OCT images for family F1 members demonstrated moderate to severe foveal atrophy. The foveal thickness of the proband F3-V4 was pathologically unremarkable (Appendix 2). Analysis of the left eye of patient F1-V5 was not available due to unsuccessful retinal detachment surgery, and the OCT of her right eye showed thinned outer retinal layers (Appendix 2). Her right eye was diagnosed with posterior subcapsular cataract (PSCC) and keratoconus. Furthermore,

patient F3-V4 was affected by PSCC and keratoconus in both eyes (Appendix 3). Disease progression was slower in family F2. The onset of central vision loss occurred at age 30 in this family; therefore, F2-V5 was not affected at age 25. His VA was  $\geq 0.3$  logMAR. The OCTs of this family showed normal or moderately thinned retinal layers, and only F2-V6 was diagnosed with PSCC (Table 1 and Appendix 2). Patient F2-V5 was prescribed daily vitamin A supplementation by an ophthalmologist between the age of 10 and 13 and daily every other month in the following time. The F1 members' lipid profiles were assessed after sequencing and segregation analyses to evaluate the clinical effects of the variant in *TTPA* (Gene ID 7274; OMIM 600415). Low-density lipoprotein (LDL) concentrations were moderately high, and high-density lipoprotein (HDL) concentrations were low (Appendix 4).

*RLBPI* was the candidate gene in the two other extended consanguineous pedigrees, families F4 and F5 (Figure 1). The initial symptom was nyctalopia at the age of 2 in both families. Although disease onset was early in life, disease progression was slow (Table 2). Members of family F4 presented partial peripheral and central vision and better paracentral vision, whereas family F5 members lost their peripheral and central vision at the age of 51 and 60 (Table 2). All members of family F4 had headaches upon sun exposure, which is associated with photophobia. Fundus examinations verified an atypical form of RP and RPA (Appendix 2). This condition is expressed through a large number of discrete, small, yellow-white dots at the level of the RPE and concentrated in the retinal midperiphery [17]. The ERG results were severely reduced (Figure 2), whereas the VAs were at the level of counting fingers (Table 2). The OCT images revealed atrophic changes at the macula (Appendix 2). Patient F5-V6 exhibited the most advanced phenotype. He lost his peripheral vision at the age of 27 and central vision at the age of 41. His current VA was only hand motion, and the OCT showed severe atrophic maculopathy. Additionally, he was the only patient diagnosed with PSCC in both eyes. Further investigations of his fundus showed no RPA, but typical RP, unlike his sister and family F4 members. This may be due to advanced retinal degeneration. All patients in this study were evaluated with slit-lamp biomicroscopy, and only F4-V13 had a congenital blue dot cataract (Table 2). The mode of inheritance for congenital blue dot cataract is often autosomal dominant, but cases of autosomal recessive and X-linked mutations have been reported [18].

*Exome sequencing and segregation analysis:* Exome sequencing was performed on the probands of the five families affected with arRP (F1-V9, F2-V5, F3-V4, F4-V13, and F5-V6; Figure 1). The mean depth across the targeted regions

TABLE 1. CLINICAL EXAMINATION RESULTS FOR PARTICIPANTS WITH RPI VARIANTS.

Index	Identified gene; HGVSaa	Age	Nyctalopia (age)	Peripheral vision loss (age)	Central vision loss (age)	VA /BCVA	Slit lamp Biomicroscopy	Keratoconus	ffERG	OCT evaluation	Further clinical evaluation data
F1-V5	RPI; p.Arg376Ter	33	Y (6)	Y (20)	Y (25)	OD: LP/NI OS: NLP/NI	OD: Mild PSCC OS: Surgical aphakia	OD: Y OS: Y	OD/ OS: Severe reduced scotopic and photopic responses	OD: Generalised thinning of the outer retinal layer OS: Post surgery	High Cholesterol high LDL
F1-V6	RPI; p.Arg376Ter	44	Y (6)	Y (20)	Y (25)	OD: LP/NI OS: NLP/NI	OD/ OS: Clear lens	OD: N OS: N	OD/ OS: Moderate to severe reduced scotopic and photopic responses	OD/ OS: Severe foveal atrophy	High triglyceride high LDL low HDL
F1-V9	RPI; p.Arg376Ter	27	Y (5)	Y (7)	Y (25)	OD:HM/NI OS:HM/NI	OD/ OS: Clear lens	OD: N OS: N	OD/ OS: Severe reduced scotopic and photopic responses	OD: Moderate foveal atrophy OS: Moderate foveal atrophy; superior retinoschisis	High LDL low HDL
F2-V5	RPI; p.Gly203Arg	25	Y (10)	Y (17)	N	OD: 0.4/0.5 OS: 0.3/0.3	OD/ OS: Clear lens	OD: N OS: N	OD/ OS: Severe reduced scotopic and photopic responses	OD: Without pathological remark OS: Mild to foveal atrophy	Vit A supplement
F2-V6	RPI; p.Gly203Arg	35	Y (5)	Y (14)	Y (30)	OD: CF 10cm/NI OS: HM/NI	OD/ OS: PSCC	OD: N OS: N	OD/ OS: Severe reduced scotopic and photopic responses	OD: Without pathological remark OS: Mild to foveal atrophy	-

Index	Identified gene; HGVSaa	Age	Nyctalopia (age)	Peripheral vision loss (age)	Central vision loss (age)	VA /BCVA	Slit lamp Biomicroscopy	Keratoconus	ffERG	OCT evaluation	Further clinical evaluation data
F3-V4	RP1; p.Gly203Arg	26	Y (5)	Y (15)	Y (22)	OD: HM / NI OS: HM/ NI	OD/ OS: PSSC operated cataract surgery	OD: Y OS: Y	Moderate to severe reduced scotopic and photopic responses	OD/ OS: Without pathological remarks	-

Y yes; N no; OD right eye; OS left eye; LP light perception; NI no improvement; NLP no light perception; HM hand motion; CF counting fingers.

TABLE 2. CLINICAL EXAMINATION RESULTS FOR PARTICIPANTS WITH RLBPI VARIANTS.

Index	Identified gene; HGVSaa	Age (age)	Nyctalopia (age)	Peripheral vision loss (age)	Central vision loss (age)	VA/ BCVA	Slit lamp Biomicroscopy	Keratocoi- nus	ffERG	OCT evaluation	Further clinical evaluation data
F4-V10	RLBPI; p.Thr27ProfsTer26	30	Y (2)	Paracentral vision better than periph- eral vision	Para- central vision better than central vision	OD:CF 1m/NI OS:CF closely/ NI	OD/OS: Clear lens	OD: N OS: N	OD/OS: Severe reduced scotopic and photopic responses	OD/OS: Atrophic maculopathy	Photophobia
F4-V11	RLBPI; p.Thr27ProfsTer26	28	Y (2)	Paracentral vision better than periph- eral vision	Para- central vision better than central vision	OD:0.05/ NI OS:0.05/ NI	OD/OS: Clear lens	OD: N OS: N	Severe reduced scotopic and photopic responses	OD/OS: Atrophic maculopathy	Photophobia
F4-V12	RLBPI; p.Thr27ProfsTer26	26	Y (2)	Paracentral vision better than periph- eral vision	Para- central vision better than central vision	OD:CF closely/ 0.1 OS:CF 2m/NI	OD/OS: Clear lens	OD: N OS: N	Severe reduced scotopic and photopic responses	OD/OS: Atrophic maculopathy	Photophobia
F4-V13	RLBPI; p.Thr27ProfsTer26	34	Y (2)	Paracentral vision better than periph- eral vision	Para- central vision better than central vision	OD:CF 2.5m/NI OS:CF 2.5m/NI	OD/OS: Congen-ital blue dots cataract	OD: N OS: N	OD/OS: Moderate to severe reduced scotopic and photopic responses	OD/OS: Atrophic maculopathy	Photophobia
F5-V5	RLBPI; p.Pro133GlnfsTer126	60	Y (2)	Y (35)	Y (50)	OD: CF closely/ NI OS: CF closely/ NI	OD/OS: Nuclear sclerosis	OD: N OS: N	OD/OS: Severe reduced scotopic and photopic responses	OD/OS: Atrophic maculopathy	-

Index	Identified gene; HGVSaa	Age	Nyctalopia (age)	Peripheral vision loss (age)	Central vision loss (age)	VA/ BCVA	Slit lamp Biomicroscopy	Keratocoanus	ffERG	OCT evaluation	Further clinical evaluation data
F5-V6	<i>RLBPI</i> ; p.Pro133GlnfsTer126	51	Y (2)	Y (27)	Y (41)	OD: HM/ NI OS: HM/NI	OD/OS: Mild PSCC	OD: N OS: N	OD/OS: Severe reduced scotopic and photopic responses	OD/ OS: Atrophic maculopathy	

Y yes; N no; OD right eye; OS left eye; CF counting fingers; NI no improvement; HM hand motion



Figure 2. Electroretinography responses of the right (OD) and left (OS) eyes for affected individuals in families F1 to F5. Each column presents a) the rod response through 0.01 cd•s/m<sup>2</sup> flashlight (dark adapted), b) the combined rod-cone response through 10.0 cd•s/m<sup>2</sup> flashlight (dark adapted), and c) the single cone response through flicker light at the 30 Hz frequency (light adapted). Electric responses are noted in a and b waves for flashlight or positive (P) and negative (N) for flicker light.

ranged from 59 to approximately 149, and all targets were covered at  $\geq 10\times$ . To identify candidate pathogenic variants, ES results were filtered based on the following criteria: (i) Out of the total variants, we filtered variants in the critical genomic regions (exons and splice sites), including loss of function and missense variants with a total read depth  $\geq 10\times$ . (ii) We filtered the disease-causing genes that are associated with retinopathies [19]. (iii) The pedigrees demonstrated an autosomal recessive mode of inheritance (Figure 1). Therefore, variants with homozygous or compound heterozygous status were prioritized. (iv) We then filtered the variants with a minor allele frequency (MAF)  $< 1\%$  in the ExAC, GnomAD, 1000 Genomes Project, and NHLBI Exome Sequencing Project (ESP; Table 3). We performed in silico prediction analyses for the filtered candidate variants using the Alamut Visual prediction software tool. These variants were further prioritized based on the information available in public variation databases, including HGMD, ClinVar, and Ensembl. The variant filtration strategy identified a total of seven variants across the five probands in five different RP genes (*RPI*, *RLPBI*, *MERTK* [Gene ID 10461; OMIM 604705], *TTPA*, and

*IFT140* [Gene ID 9742; OMIM 614620]), all of which were homozygous (Table 4). To further assess the candidate variants, segregation analyses were performed in the affected and available unaffected family members (Figure 1 and Figure 3). This led us to determine the disease-causing variants in each family (Table 4). For family F1, the variant in *RPI* (c.1126C>T; p.Arg376Ter) segregated in the homozygous state with RP in affected family members and the *RPI* missense variant (c.607G>A; p.Gly203Arg) was found in families F2 and F3. Two disease-causing frameshift variants in *RLPBI* were responsible for RPA in families F4 and F5 (c.79delA, p.Thr27ProfsTer26 and c.398delC, p.Pro133GlnfsTer126), respectively. Both variants were observed to segregate in the homozygous state with the disease in the affected members, while heterozygous carriers were unaffected. For family F5, segregation analysis was available for one sibling.

## DISCUSSION

The pedigrees for the five participating families demonstrated an autosomal recessive RP inheritance pattern (Figure 1). The disease was diagnosed in every affected member

TABLE 3. EXOME SEQUENCING RESULTS AFTER FILTERING FOR CANDIDATE VARIANTS.

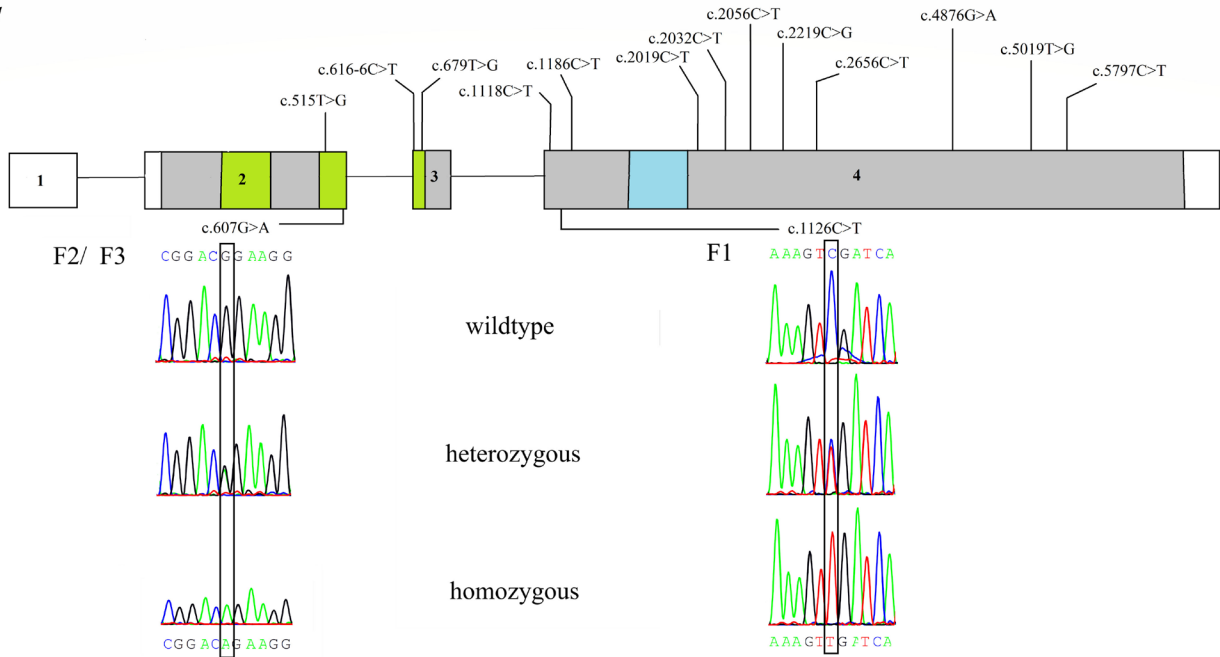
Filtering steps	F1	F2	F3	F4	F5
Total variant number	66638	67914	61992	65974	68432
Coding/ splice site region; read depth $\geq 10$	13853	14165	12843	13769	14264
Associated with retinopathies	266	275	241	324	285
Homozygous/ compound heterozygous	125	115	127	117	116
MAF $\leq 1\%$	2	1	2	2	1

TABLE 4. CLASSIFICATION OF CANDIDATE GENES AND THEIR VARIANTS.

Family No.	Gene	Variant coordinate (hg19)	RefSeq	Exon	HGVS cDNA	HGVS aa	Consequences	ClinVar	Segregation analysis		ACMG classification	ACMG criteria
									RP affected	RP unaffected		
F1	RPI	chr8:55537568	NM_006269.1	43925	c.1126C>T	p.Arg376Ter	Nonsense	NA	43893	0/3	Pathogenic	PVSI, PM2, PPI
F1	TTPA	chr8:63976829	NM_000370.3	43926	c.599C>T	p.Pro200Leu	Missense	NA	43893	43833	VUS	Other criteria are not met
F2/F3	RPI	chr8:55534133	NM_006269.1	43865	c.607G>A	p.Gly203Arg	Missense	LP rs786205589	F2: 2/2 F3: 3/3	F2: 0/3 F3: 0/2	LP	PM2, PM3, PPI, PP3
F3	MERTK	chr2:112686733	NM_006343.2	43880	c.98C>T	p.Pro33Leu	Missense	NA	NA	NA	VUS	Other criteria are not met
F4	RLBPI	chr15:89761858	NM_000326.4	43930	c.79delA	p.Thr27ProfsTer26	Frameshift-deletion	Pathogenic rs1567124404	43925	0/3	Pathogenic	PVSI, PM2, PPI
F4	IFT140	chr16:1569962-1569967	NM_014714.3	29/31	c.3955_3960 delGCCAAG	p.Ala1319 Lys1320del	Frameshift-deletion	VUS <sup>1</sup> /LP <sup>2</sup> rs746697405	43834	0/3	VUS	Other criteria are not met
F5	RLBPI	chr15:89758418	NM_000326.4	43991	c.398delC	p.Pro133Gln	Frameshift-deletion	NA	43863	0/1	Pathogenic	PVSI, PM2, PPI

NA: not available, LP: likely pathogenic, VUS: variant of unknown significance, Renal dysplasia, retinal pigmentary dystrophy, cerebellar ataxia and skeletal dysplasia. Orofacial-digital syndrome III, Short-rib thoracic dysplasia I with or without polydactyly

**A: *RPI***



**B: *RLBPI***

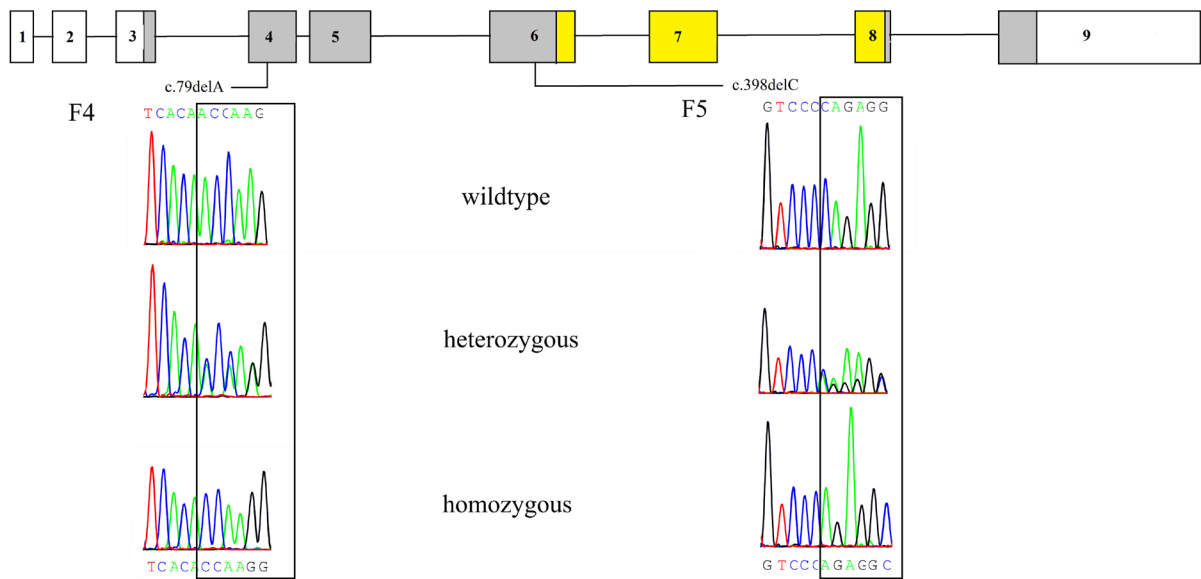


Figure 3. Pathogenic *RPI* and *RLBPI* variants. The genes are schematically represented and previously reported as retinitis pigmentosa (RP)-causing nonsense or missense variants marked in *RPI*. The exons are numbered; white parts indicate non-coding regions, and gray parts indicate coding regions. **A:** The *RPI* gene doublecortin (DCX) domain is marked in green, and the *Drosophila melanogaster* bifocal (BIF) domain is marked in blue. **B:** Yellow indicates the retinal-binding domain in *RLBPI*. The variants of this study are beneath every gene schema with Sanger chromatograms of unaffected heterozygous, and affected homozygous individuals. Nucleotide variations are circled.

of the five consanguineous Jordanian families. The initial symptoms were nyctalopia and decreased VA. The subjects showed phenotypic heterogeneity, depending on the causative genes. The fundus examinations revealed different subtypes of RP: typical RP in families F1, F2, and F3 for whom we

identified variants in *RPI* and RPA in families F4 and F5 in whom we identified variants in *RLBPI*. In cases of typical RP, the disease starts with nyctalopia in the first decade of life, followed by peripheral vision loss (second decade) and central vision loss (third decade). Disease progression was

slower in patients from family F2. Patient F2-V5 has been treated with continuous vitamin A supplementation for 15 years. It was reported in the literature that vitamin A supplementation could have positive effects on the visual field or the retina electrophysiology, or on both, depending on the patient's genotype [20]. Further studies on the positive effects of vitamin A on the retina must be conducted, and its effects cannot be confirmed in this case. For all participants, the ffERG confirmed the early dysfunction of retinal photoreceptors, but it did not correlate with the disease severity in its advanced stages. RP severity was presented in the VA, BCVA, and OCT images (Table 1 and Appendix 2). Across the five participating families, PSCC or keratoconus was present in some of the affected individuals (Appendix 3, Table 1, and Table 2). It has been reported that keratoconus correlates with hereditary retinal dystrophies, including RP [21].

Through ES, we identified two variants in the *RPI* gene for participants affected by typical RP and verified them with Sanger sequencing. Oxygen-regulated photoreceptor 1 (*RPI*; OMIM 603937), which is located on chromosome 8 (8q11.2-q12.1), consists of four exon regions, and encodes a 2,156-amino acid protein [22]. Mouse models and human tissue analysis revealed that *RPI* is differentially expressed in the photoreceptor outer segment architecture and is localized in connecting cilia rods and cones [23,24]. The protein encoded by *RPI* plays a role in transporting proteins between the inner and outer segments of the photoreceptors where it participates in regulating c-Jun N-terminal kinase (JNK) signaling cascades [24]. As reported in RetNet, variants in *RPI* cause 5% to 10% of the arRP cases [25]. Eighty-three pathogenic and likely pathogenic variants, including frameshift, missense, and nonsense variants, have been identified in *RPI* (ClinVar). Pathogenic and likely pathogenic variants are mostly located in exon 4 [27]. In family F1, we identified a homozygous nonsense variant in the last *RPI* exon (c.1126C>T; p.Arg376Ter; Figure 1, Table 4). This variant was previously reported to cause arRP in a Pakistani pedigree [28]. The highest MAF for this variant were 0.013% (gnomAD) and 0.01213% (ExAC) in the South Asian population (Appendix 5). Segregation analysis showed that *RPI* (c.1126C>T; p.Arg376Ter) is homozygous in the affected individuals only and heterozygous in the unaffected family members (Figure 1, Table 4, Figure 3). We excluded the candidate variant in the *TTPA* gene after segregation analysis for being homozygous in an unaffected family member. However, elevated LDL and lower HDL concentrations might be related to impaired vitamin E function caused by the variant in *TTPA* [29].

In families F2 and F3, the ES results identified another previously reported missense variant in *RPI* (c.607G>A; p.Gly203Arg; Figure 1, Table 4). This variant has been reported in the Iranian population to cause arRP [30]. It is conserved across various related species (Alamut Visual Software; Orthologs Ensemble; Appendix 6). In silico analysis tools predict this variant to be disease-causing. It is currently classified in ClinVar as likely pathogenic (rs786205589). The validation and segregation analyses showed that five patients in families F2 and F3 were homozygous for *RPI* (c.607G>A; p.Gly203Arg), and their unaffected relatives were not (Figure 1 and Figure 3). The present analyses further supported a disease-causing role for this variant.

Clinical investigations for families F4 and F5 revealed a form of atypical RP: RPA. Those clinical manifestations differed from the RP phenotypes in families F1, F2, and F3. The disease onset was at an earlier age, 2 years old, but with slower vision deterioration. All affected subjects in family F4 were 26 to 34 years old and still had peripheral and central vision. The older proband of family F5 presented peripheral vision loss at the age of 35 years and central vision loss at the age of 50. Compared with the affected individuals in family F5, F5-V6 presented fewer symptoms of RPA, and his retinal degeneration was faster (Table 2). This suggests variable expressivity among the affected individuals within the same family. This finding also suggests that RPA could be correlated with slower disease deterioration.

We identified variants in *RLBPI* to be disease-causing in families F4 and F5. Retinaldehyde-binding protein 1 (*RLBPI*) on chromosome 15 (15q26.1) contains nine exonic and seven intronic regions and is translated to the 36-kD cellular retinaldehyde-binding protein (CRALBP) [31,32]. It is part of the retinal pigment epithelium (RPE) in photoreceptors, Müller cells, and ganglion cells, and functions in the visual cycle [33]. As a carrier for 11-cis-retinol and 11-cis-retinal, *RLBPI* supports chromophore recycling in rods and cones [34]. Variants in the *RLBPI* gene have been reported to cause IRDs, such as RPA, Bothnia-type dystrophy (BD), Newfoundland rod-cone dystrophy (NFRCD), RP, and fundus albipunctatus (FA) [25]. Forty-one variants have been reported in ClinVar as pathogenic or likely pathogenic. Family F4 presented an extended pedigree, with members affected by arRP in three generations (Figure 1). We performed ES for the proband F4-V13 and identified the candidate gene, *RLBPI* (c.79delA; p.Thr27ProfsTer26). This *RLBPI* frameshift variant causes a premature termination signal. Segregation analysis identified the five affected members of family F4 to be homozygous for this variant, while the unaffected parents and one sibling were heterozygous (Figure 1, Table 4, and Figure 3). Moreover, the

variant (c.79delA; p. Thr27ProfsTer26) is listed in ClinVar as pathogenic (rs1567124404).

In this study, we detected a novel frameshift variant in *RLBPI* (c.398delC; p.Pro133GlnfsTer126) as disease-causing in family F5 (Table 4). This variant segregated in the affected members and was heterozygous in the unaffected sibling (Figure 1, Table 3, and Figure 3). Furthermore, we classified the ophthalmic outcome as likely RPA-causative.

**Conclusion:** In this study, we identified a novel pathogenic variant in *RLBPI* (c.398delC; p.Pro133GlnfsTer126) and three recurrent variants in the *RPI* and *RLBPI* genes. We thoroughly investigated their consequent clinical manifestations using a battery of ophthalmic tests. We described heterogenic disease phenotypes of RP depending on the affected genes: typical RP for variants in *RPI* and RPA for variants in *RLBPI*. This study also demonstrated that ES is a valuable ophthalmic molecular diagnostic tool and expands the causative variant spectrum in patients with RP. Genetic analyses enable us to perform targeted diagnostic testing and identify therapeutic approaches for gene therapy.

#### APPENDIX 1. PRIMER SEQUENCES FOR SANGER SEQUENCING.

To access the data, click or select the words “[Appendix 1.](#)”

#### APPENDIX 2. FUNDUS AND OCT IMAGES FOR F1-F5 MEMBERS.

To access the data, click or select the words “[Appendix 2.](#)”

#### APPENDIX 3. PENTACAM IMAGES FOR THE RIGHT (OD) AND LEFT (OS) EYES FOR FAMILIES F1 TO F5.

To access the data, click or select the words “[Appendix 3.](#)”

#### APPENDIX 4. LIPID PROFILING OF FAMILY F1 MEMBERS.

To access the data, click or select the words “[Appendix 4.](#)”

#### APPENDIX 5. MINOR ALLELE FREQUENCIES (MAF) AND IN SILICO PREDICTIONS CANDIDATE VARIANTS.

To access the data, click or select the words “[Appendix 5.](#)”

#### APPENDIX 6. AMINO ACID CONSERVATION FOR CANDIDATE MISSENSE AND FRAMESHIFT VARIANTS ACROSS RELATED SPECIES USING ALAMUT VISUAL PREDICTION SOFTWARE. THE MISSENSE VARIANTS ARE TTPA (C.599C>T) AND RP1 (C.607G>A). THE FRAMESHIFT VARIANT IS IFT140 (C.3955\_3960DELGCCAAG).

To access the data, click or select the words “[Appendix 6.](#)”

#### ACKNOWLEDGMENTS

Supported by a grant from the Deanship of Academic Research at the University of Jordan (Grant No. 2013/39), Abdul Hameed Shoman Foundation (Grant No. 2017/05), Amman, Jordan. Neither of the funders had any role in the data collection, analysis, interpretation, or manuscript writing. Dr. Belal Azab ([azabbm@mymail.vcu.edu](mailto:azabbm@mymail.vcu.edu)) and Dr. Abdalla Awidi ([abdalla.awidi@gmail.com](mailto:abdalla.awidi@gmail.com)) are co-corresponding authors for this paper.

#### REFERENCES

- Hamel C. Retinitis pigmentosa. Orphanet J Rare Dis 2006; 1:40-[\[PMID: 17032466\]](#).
- Bravo-Gil N, Gonzalez-Del Pozo M, Martin-Sanchez M, Mendez-Vidal C, Rodriguez-de la Rúa E, Borrego S, Antinolo G. Unravelling the genetic basis of simplex Retinitis Pigmentosa cases. Sci Rep 2017; 7:41937-[\[PMID: 28157192\]](#).
- Parmeggiani F, Sato G, De Nadai K, Romano MR, Binotto A, Costagliola C. Clinical and Rehabilitative Management of Retinitis Pigmentosa: Up-to-Date. Curr Genomics 2011; 12:250-9. [\[PMID: 22131870\]](#).
- Na KH, Kim HJ, Kim KH, Han S, Kim P, Hann HJ, Ahn HS. Prevalence, Age at Diagnosis, Mortality, and Cause of Death in Retinitis Pigmentosa in Korea-A Nationwide Population-based Study. Am J Ophthalmol 2017; 176:157-65. [\[PMID: 28130043\]](#).
- Nangia V, Jonas JB, Khare A, Sinha A. Prevalence of retinitis pigmentosa in India: the Central India Eye and Medical Study. Acta ophthalmologica. 2012; 90:e649-50. [\[PMID: 22594809\]](#).
- Chizzolini M, Galan A, Milan E, Sebastiani A, Costagliola C, Parmeggiani F. Good epidemiologic practice in retinitis pigmentosa: from phenotyping to biobanking. Curr Genomics 2011; 12:260-6. [\[PMID: 22131871\]](#).
- Deshpande R, Save P, Deshpande M, Shegunashi M, Chougule M, Khandekar R. Validity and cost-effectiveness of cone adaptation test as a screening tool to detect retinitis pigmentosa. Oman J Ophthalmol 2016; 9:135-8. [\[PMID: 27843226\]](#).
- Hartong DT, Berson EL, Dryja TP. Retinitis pigmentosa. Lancet (London, England) 2006; 368:1795-809. [\[PMID: 17113430\]](#).

9. Brancati N, Frucci M, Gragnaniello D, Riccio D, Di Iorio V, Di Perna L. Automatic segmentation of pigment deposits in retinal fundus images of retinitis pigmentosa. *Comput Med Imaging Graph* 2018; 66:73-81. [PMID: 29573581].
10. Mrejen S, Audo I, Bonnel S, Sahel JA. Retinitis Pigmentosa and Other Dystrophies. *Dev Ophthalmol* 2017; 58:191-201. [PMID: 28351048].
11. Chang S, Vaccarella L, Olatunji S, Cebulla C, Christoforidis J. Diagnostic challenges in retinitis pigmentosa: genotypic multiplicity and phenotypic variability. *Curr Genomics* 2011; 12:267-75. [PMID: 22131872].
12. Moore AT, Fitzke F, Jay M, Arden GB, Inglehearn CF, Keen TJ, Bhattacharya SS, Bird AC. Autosomal dominant retinitis pigmentosa with apparent incomplete penetrance: a clinical, electrophysiological, psychophysical, and molecular genetic study. *Br J Ophthalmol* 1993; 77:473-9. [PMID: 8025041].
13. Goldenberg-Cohen N, Banin E, Zalstein Y, Cohen B, Rotenstreich Y, Rizel L, Basel-Vanagaite L, Ben-Yosef T. Genetic heterogeneity and consanguinity lead to a “double hit”: homozygous mutations of MYO7A and PDE6B in a patient with retinitis pigmentosa. *Mol Vis* 2013; 19:1565-71. [PMID: 23882135].
14. Sharon D, Ben-Yosef T, Goldenberg-Cohen N, Pras E, Gradstein L, Soudry S, Mezer E, Zur D, Abbasi AH, Zeitz C, Cremers FPM, Khan MI, Levy J, Rotenstreich Y, Birk OS, Ehrenberg M, Leibur R, Newman H, Shomron N, Banin E, Perlman I. A nationwide genetic analysis of inherited retinal diseases in Israel as assessed by the Israeli inherited retinal disease consortium (IIRDC). *Hum Mutat* 2020; 41:140-9. [PMID: 31456290].
15. Hamel C. Retinitis Pigmentosa. *Orphanet J Rare Dis* 2006; 1:40-[PMID: 17032466].
16. Gonzalez-Del Pozo M, Fernandez-Suarez E, Martin-Sanchez M, Bravo-Gil N, Mendez-Vidal C, Rodriguez-de la Rúa E, Borrego S, Antiñolo G. Unmasking Retinitis Pigmentosa complex cases by a whole genome sequencing algorithm based on open-access tools: hidden recessive inheritance and potential oligogenic variants. *J Transl Med* 2020; 18:73-[PMID: 32050993].
17. Hipp S, Zobor G, Glockle N, Mohr J, Kohl S, Zrenner E, Weisschuh N, Zobor D. Phenotype variations of retinal dystrophies caused by mutations in the RLBPI gene. *Acta ophthalmologica*. 2015; 93:e281-6. [PMID: 25429852].
18. Berry V, Ionides AC, Moore AT, Bhattacharya SS. A novel locus for autosomal dominant congenital cerulean cataract maps to chromosome 12q. *European journal of human genetics* *Eur J Hum Genet* 2011; 19:1289-91. [PMID: 21731060].
19. Azab B, Barham R, Ali D, Dardas Z, Rashdan L, Bijawi M, Maswadi R, Awidi A, Jafar H, Abu-Ameerh M, Al-Bdour M, Amr S, Awidi A. Novel CERKL variant in consanguineous Jordanian pedigrees with inherited retinal dystrophies. *Can J Ophthalmol* 2019; 54:51-9. [PMID: 30851774].
20. Berson EL, Weigel-DiFranco C, Rosner B, Gaudio AR, Sandberg MA. Association of Vitamin A Supplementation With Disease Course in Children With Retinitis Pigmentosa. *JAMA Ophthalmol* 2018; 136:490-5. [PMID: 29596553].
21. Bakkar MM, Alzghoul EA, Haddad MF. Clinical characteristics and causes of visual impairment in a low vision clinic in northern Jordan. *Clin Ophthalmol* 2018; 12:631-7. [PMID: 29662299].
22. Pierce EA, Quinn T, Meehan T, McGee TL, Berson EL, Dryja TP. Mutations in a gene encoding a new oxygen-regulated photoreceptor protein cause dominant retinitis pigmentosa. *Nat Genet* 1999; 22:248-54. [PMID: 10391211].
23. Goldberg AF, Moritz OL, Williams DS. Molecular basis for photoreceptor outer segment architecture. *Prog Retin Eye Res* 2016; 55:52-81. [PMID: 27260426].
24. Liu Q, Zhou J, Daiger SP, Farber DB, Heckenlively JR, Smith JE, Sullivan LS, Zuo J, Milam AH, Pierce EA. Identification and subcellular localization of the RP1 protein in human and mouse photoreceptors. *Invest Ophthalmol Vis Sci* 2002; 43:22-32. [PMID: 11773008].
25. . SP Daiger BR. J Greenberg, A Christoffels, W Hid. RetNet: genes and Mapped Loci Causing Retinal Diseases *Invest. Ophthalmol.Vis. Sci.* 1998; 39:S295-.
26. Nanda A, McClements ME, Clouston P, Shanks ME, MacLaren RE. The Location of Exon 4 Mutations in RP1 Raises Challenges for Genetic Counseling and Gene Therapy. *Am J Ophthalmol* 2019; 202:23-9. [PMID: 30731082].
27. Li L, Chen Y, Jiao X, Jin C, Jiang D, Tanwar M, Ma Z, Huang L, Ma X, Sun W, Chen J, Ma Y, M'hamdi O, Govindarajan G, Cabrera PE, Li J, Gupta N, Naeem MA, Khan SN, Riazuddin S, Akram J, Ayyagari R, Sieving PA, Riazuddin SA, Hejtmancik JF. Homozygosity Mapping and Genetic Analysis of Autosomal Recessive Retinal Dystrophies in 144 Consanguineous Pakistani Families. *Invest Ophthalmol Vis Sci* 2017; 58:2218-38. [PMID: 28418496].
28. Terasawa Y, Ladha Z, Leonard SW, Morrow JD, Newland D, Sanan D, Packer L, Traber MG, Farese RV Jr. Increased atherosclerosis in hyperlipidemic mice deficient in alpha-tocopherol transfer protein and vitamin E. *Proc Natl Acad Sci USA* 2000; 97:13830-4. [PMID: 11095717].
29. Eisenberger T, Neuhaus C, Khan AO, Decker C, Preising MN, Friedburg C, Bieg A, Gliem M, Charbel Issa P, Holz FG, Baig SM, Hellenbroich Y, Galvez A, Platzer K, Wollnik B, Laddach N, Ghaffari SR, Rafati M, Botzenhart E, Tinschert S, Börger D, Bohring A, Schreml J, Körtge-Jung S, Schell-Apacik C, Bakur K, Al-Aama JY, Neuhann T, Herkenrath P, Nürnberg G, Nürnberg P, Davis JS, Gal A, Bergmann C, Lorenz B, Bolz HJ. Increasing the yield in targeted next-generation sequencing by implicating CNV analysis, non-coding exons and the overall variant load: the example of retinal dystrophies. *PLoS One* 2013; 8:e78496-[PMID: 24265693].
30. Sparkes RS, Heinzmann C, Goldflam S, Kojis T, Saari JC, Mohandas T, Klisak I, Bateman JB, Crabb JW. Assignment of the gene (RLBP1) for cellular retinaldehyde-binding protein (CRALBP) to human chromosome 15q26 and mouse chromosome 7. *Genomics* 1992; 12:58-62. [PMID: 1733864].

31. Intres R, Goldflam S, Cook JR, Crabb JW. Molecular cloning and structural analysis of the human gene encoding cellular retinaldehyde-binding protein. *J Biol Chem* 1994; 269:25411-8. [PMID: 7929238].
32. Wen B, Li S, Li H, Chen Y, Ma X, Wang J, Lu F, Qu J, Hou L. Microphthalmia-associated transcription factor regulates the visual cycle genes Rlbp1 and Rdh5 in the retinal pigment epithelium. *Sci Rep* 2016; 6:21208-[PMID: 26876013].
33. Saari JC, Nawrot M, Kennedy BN, Garwin GG, Hurley JB, Huang J, Possin DE, Crabb JW. Visual cycle impairment in cellular retinaldehyde binding protein (CRALBP) knockout mice results in delayed dark adaptation. *Neuron* 2001; 29:739-48. [PMID: 11301032].

Articles are provided courtesy of Emory University and the Zhongshan Ophthalmic Center, Sun Yat-sen University, P.R. China. The print version of this article was created on 19 June 2020. This reflects all typographical corrections and errata to the article through that date. Details of any changes may be found in the online version of the article.